Cardiovascular Research (2017) **113**, 508–518
doi:10.1093/cvr/cvx021

New insights into shear stress-induced endothelial signalling and barrier function: cell-free fluid versus blood flow

Sulei Xu[1], Xiang Li[1], Kyle Brian LaPenna[1], Stanley David Yokota[2], Sabine Huke[3], and Pingnian He[1]*

[1]Department of Cellular and Molecular Physiology, College of Medicine, Pennsylvania University, 500 University Drive, Hershey, PA 17033, USA; [2]Department of Physiology and Pharmacology, School of Medicine, West Virginia University, One Medical Center Drive, Morgantown, WV 26506, USA; and [3]Department of Medicine, University of Alabama at Birmingham, 901 19th street South. Birmingham, AL 35294, USA

Received 14 June 2016; revised 28 November 2016; editorial decision 17 January 2017; accepted 27 January 2017; online publish-ahead-of-print 27 February 2017

Time for primary review: 44 days

Aims Fluid shear stress (SS) is known to regulate endothelial cell (EC) function. Most of the studies, however, focused on the effects of cell-free fluid-generated wall SS on ECs. The objective of this study was to investigate how changes in blood flow altered EC signalling and endothelial function directly through wall SS and indirectly through SS effects on red blood cells (RBCs).

Methods and results Experiments were conducted in individually perfused rat venules. We experimentally induced changes in SS that were quantified by measured flow velocity and fluid viscosity. The concomitant changes in EC $[Ca^{2+}]_i$ and nitric oxide (NO) were measured with fluorescent markers, and EC barrier function was assessed by fluorescent microsphere accumulation at EC junctions using confocal imaging. EC eNOS activation was evaluated by immunostaining. In response to changes in SS, increases in EC $[Ca^{2+}]_i$ and gap formation occurred only in blood or RBC solution perfused vessels, whereas SS-dependent NO production and eNOS-Ser^{1177} phosphorylation occurred in both plasma and blood perfused vessels. A bioluminescent assay detected SS-dependent ATP release from RBCs. Pharmacological inhibition and genetic modification of pannexin-1 channels on RBCs abolished SS-dependent ATP release and SS-induced increases in EC $[Ca^{2+}]_i$ and gap formation.

Conclusions SS-induced EC NO production occurs in both cell free fluid and blood perfused vessels, whereas SS-induced increases in EC $[Ca^{2+}]_i$ and EC gap formation require the presence of RBCs, attributing to SS-induced pannexin-1 channel dependent release of ATP from RBCs. Thus, changes in blood flow alter vascular EC function through both wall SS and SS exerted on RBCs, and RBC released ATP contributes to SS-induced changes in EC barrier function.

Keywords Shear stress • Endothelial calcium • Nitric oxide • Microvessel permeability • ATP

1. Introduction

In the circulatory system, sustained fluid shear stress (SS) plays an important role in maintaining vascular wall endothelium integrity, and local perturbations in hemodynamic flow patterns contribute to the pathogenesis of vascular dysfunction.[1] Most of the SS-related studies have been conducted in cultured endothelial monolayers in the absence of blood cell components. Although these studies provided insights into the mechanisms of SS generated responses,[2–8] cultured endothelial cells (ECs) grown under static conditions usually have 10–100 times higher baseline permeability compared to intact microvessels, and exhibit a pro-inflammatory phenotype.[9] Therefore, their responses to mechanical forces may not fully replicate *in vivo* conditions. Additionally, the fluid in the vascular system is not a cell-free fluid. It contains blood cells that are also subject to SS under flow conditions. Studies on red blood cells (RBCs) have indicated that SS plays an important role in triggering RBCs to release bioactive agents, such as ATP.[10–14] However, previous studies of the effects of SS, either in cultured EC monolayers, in large artery segments, or in individually perfused microvessels,[15–18] have all been conducted in the absence of RBCs, whereas the studies of the effects of SS

* Corresponding author. Tel: 717 531 3596; fax: 717 531 7667, E-mail: pinghe@hmc.psu.edu

on RBCs have not involved vascular endothelium.[10–14] To date, how changes in blood flow, i.e. in the presence of RBCs, affect EC signalling and barrier function has not been studied and is essentially unknown. The effects of SS on ECs, even in the absence of blood cells, have yielded conflicting results, especially related to SS-induced changes of EC $[Ca^{2+}]_i$, the Ca^{2+} dependence of SS-induced nitric oxide (NO) production, and the effect of changing SS on microvessel permeability.[7,8,15–20] Capillaries and small venules are the main sites for fluid and solute exchange between blood and surrounding tissues, and post-capillary venules are highly susceptible to inflammation with increased permeability under pathological conditions. It is important to understand how the changes in hemodynamic forces affect the exchange function and EC barrier integrity in venules. The objective of this study is to clarify the conflicting issues in the field and provide a better understanding of blood flow-induced changes in EC signalling and barrier function in intact venules. We quantitatively measured SS-induced changes in EC $[Ca^{2+}]_i$, NO production, eNOS phosphorylation, and EC barrier integrity, and compared the responses when vessels were perfused with cell-free fluid, whole blood, or RBC solution. Our studies revealed an integrative interaction between RBCs and ECs that has been overlooked for decades in studies of SS-induced changes in EC function, and differentiated the contributions of changing wall SS from that of shear-induced release of ATP from RBCs to the alterations of microvascular EC signalling and barrier function in intact microvessels.

2. Methods

2.1 Animal preparation

Experiments were carried out on mesenteric venules (40–45 μm diameter) from female Sprague-Dawley rats (2–3-months old, 220–250 g body wt). All protocols were in accordance with guidelines of and approved by the Animal Care and Use Committee of West Virginia University (12-0707) or Pennsylvania State University (D16-00024) and National Institutes of Health (the 8th Edition, NRC 2011). Sodium pentobarbital (65 mg/kg) or inactin hydrate (180 mg/kg) was used for anaesthesia and given subcutaneously. The appropriate plane of anaesthesia is determined by the losses toe pinch response and the righting reflex. Each experiment was performed on a single vessel with one experiment per animal. Euthanasia was performed through bilateral thoracotomy while animals were under anaesthesia. Details see Supplementary material online.

2.2 Quantification of SS in individually perfused venules

Wall SS is determined by shear rate and viscosity. Wall Shear rate (γ), determined by mean fluid velocity (V_{mean}) and vessel diameter (D), is calculated by the equation $\gamma = 8V_{mean}/D$.[21] A Photron-FASTCAM high-speed camera was used to record images at 500 frames/s for flow velocity measurements. ImageJ software with the MTrackJ plugin was used to quantify the centre line RBC velocity (Vmax), the maximum velocity in laminar flow parabolic profile. The mean fluid velocity (Vmean) is calculated as Vmax/1.6.[21] Perfusate viscosity was measured using a Wells-Brookfield cone/plate digital viscometer (LVTDCP). In each experiment, a single venule was cannulated with a glass micropipette and perfused with albumin-Ringer solution (control) or other perfusates. Hydrostatic pressure, controlled by a water manometer, was applied through the micropipette to the microvessel lumen to control the flow rate. The changes in wall SS were achieved by increasing perfusion pressure from balance pressure (10–15 cm H_2O) to the desired pressure based on the viscosity of each perfusate. The measurements started immediately following the pressure change and the same SS was maintained throughout the period of measurement at each SS level.

2.3 Measurements of endothelial $[Ca^{2+}]_i$

Endothelial $[Ca^{2+}]_i$ was measured in individually perfused microvessels using the fluorescent Ca^{2+} indicator fura 2-AM. A Nikon Fluor lens (×20, NA 0.75) and a Nikon photometry system were used to record fluorescence intensity (FI). A segment of fura 2-AM-loaded vessel, at least 100 μm away from the cannulation site assuring laminar flow, was positioned within the field of view of the measuring window. The ratios of the two FI values were converted to Ca^{2+} concentrations based on an *in vitro* calibration. Details have been reported[22] and in Supplementary material online.

2.4 Measurements of endothelial NO

Endothelial NO production was measured in DAF-2 DA loaded vessels using fluorescence imaging collected by a 12-bit digital CCD camera (ORCA; Hamamatsu) using Metafluor software (Universal Imaging, West Chester, PA) and a Nikon Fluor lens (×20, NA 0.75). Each vessel was first perfused with albumin-Ringer solution containing DAF-2 DA (5 μM). Image collection started after 40 min of DAF-2 DA perfusion. Quantitative analysis was conducted at the individual EC level with selected regions of interest (ROI) along the vessel wall. SS-induced changes in FI_{DAF} were expressed as arbitrary units (AU). The NO production rate, dFI/dt, was derived by first differential conversion of cumulative FI_{DAF} over time. Details have been described previously,[23] and in the Supplementary material online. To validate the increased DAF FI as an indication of NO production, in one group of studies, a NOS inhibitor, L-NMMA (0.5 mM), was added to each of the perfusate in the entire experiment period including DAF-2 loading. The inhibited portion of DAF-2 FI by L-NMMA is considered as the quantity attributable to NO synthesis. More details are in Supplementary material online.

2.5 RBC preparation and ATP measurement

Blood was draw from a carotid artery (rat) or via cardiac puncture (mouse, wild type and Pannexin 1-deficient homozygous C57BL/6 mice, details see Supplementary material online) with heparin (20 unit/mL) and was used immediately. Platelet rich plasma was obtained by centrifugation of whole blood at 100 *g* for 15 min. To obtain RBCs, the blood was diluted in mammalian Ringer's solution and centrifuged at 500 *g* for 5 min three times with buffy coat removed. Packed RBCs were resuspended in 1% albumin-Ringer's solution at 40% haematocrit. Immediately following exposure to SS in the viscometer, RBCs or platelet rich plasma were mixed 50/50 with the luciferin/luciferase assay mix (Sigma). The light level of each sample was the mean of 20 replicate measures in 20 s using a luminometer (AutoLumatPlus LB953, Berthold). The ATP level was calculated based on the calibration curve.

2.6 Immunostaining and confocal imaging

The mesentery bearing the perfused vessel was fixed with paraformaldehyde, followed by permeabilization with 0.1% Triton X-100 before exposure to the anti-phosphorylated eNOS at Ser^{1177} (Abcam) or Thr^{495} (Cell Signalling Technology) antibody. The tissue was then incubated with Alexa 488-conjugated secondary antibody (Invitrogen) at room temperature for 2 h. Confocal images were obtained using a Leica

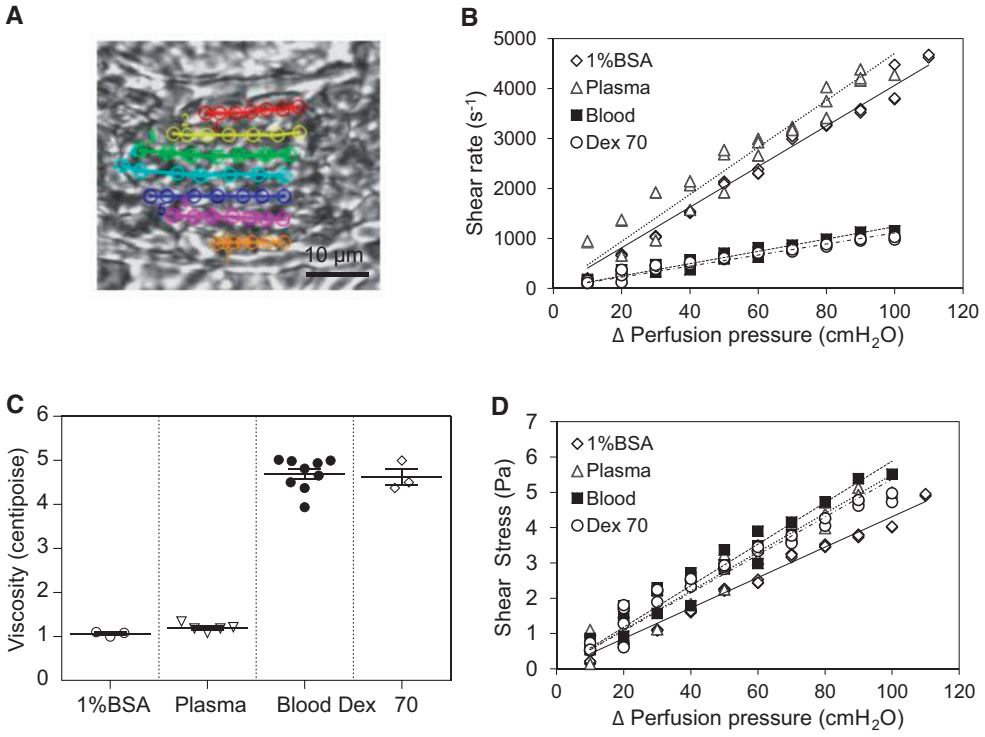

Figure 1 Quantification of wall SS in intact venules. (*A*) One of the images of a blood perfused venule captured at 500 frames/s with tracking profile of RBC velocity. (*B*) Changes of shear rate as a function of perfusion pressure with different perfusates in a 40 μm diameter venule. (*C*) Summary of viscosity measurements ($n = 9$ whole blood; $n = 5$ plasma; $n = 3$ Dextran 70). (*D*) Changes of SS as a function of perfusion pressure ($n = 3$ per group).

objective ×63 (HCX PL APO, NA 1.2) with × 1.5 electronic zoom and 0.3 μm vertical step. The FI of each vessel from each animal was the mean of 19–40 ECs and the FI of individual ECs was the mean of three selected ROIs within each cell and averaging the Z-axis stack of each ROI using Leica confocal software.[24]

2.7 Visualization of endothelial gap formation in intact microvessels

We used fluorescent microspheres (FMs) as the marker to identify endothelial gap formation. Briefly, each microvessel was perfused with a perfusate containing red FMs (100 nm, 3.6×10^{11}/mL) for 10 min with and without changing SS. Confocal images were collected after the free FMs in the vessel lumen were removed by albumin-Ringer perfusion. A stack of confocal images was obtained from each vessel at successive X-Y focal planes with vertical depth of 0.5 μm using Leica ×25 (NA 0.95) objective. The FM accumulation at EC junctions was analysed from lower half of the Z-axis image stack of the vessel. The total FI of FM (area × depth × mean intensity/pixel) was quantified as total intensity/surface area of the vessel wall under control or shear conditions. Details have been described previously.[25]

2.8 Solutions and reagents

Mammalian Ringer's solution was used for the experiments. The composition of the mammalian Ringer's solution and the sources of testing agents were described in Supplementary material online. All of the perfusates containing the test reagents were freshly prepared before each cannulation.

2.9 Data analysis and statistics

All values are means ± SE. Paired student's *t*-test was used for paired experiments conducted in the same vessel and unpaired student's *t*-test was used between group data analysis (two tails). ANOVA was used to compare data among groups. A probability value of $P < 0.05$ was considered statistically significant.

3. Results

3.1 Quantification and modulation of wall SS in individually perfused venules

The wall SS in individually perfused venules was quantified with measured viscosity and the shear rate of each perfusate under different perfusion pressures. *Figure 1A* shows one of the images used for velocity measurements in a blood perfused vessel. The mean viscosity of each perfusate (*Figure 1C*), measured at shear rate of 225 s^{-1} at 37°C, was 4.7 ± 0.12 cP for whole blood (mean haematocrit 45.0 ± 0.74%, $n = 9$), 1.2 ± 0.04 cP for rat plasma (mean protein level 5.8 ± 0.1 g/dL, $n = 5$), and 4.6 ± 0.13 cP for 10% Dextran 70 in 1% BSA solution ($n = 3$). With a relatively constant vessel diameter (≅ 40 μm), the relationship between the net perfusion pressure and shear rate (*Figure 1B*) or SS (*Figure 1D*) with each perfusate is relatively linear ($n = 3$ per group). Based on simulation models[14,26–28] the blood apparent viscosity that varies with shear rate could be 20–40% smaller than that measured at shear rate of 225 s^{-1} when the vessel was perfused with whole blood or 40% RBCs at a higher shear rate. We also expect that the perfused RBCs were exposed to a higher SS than the

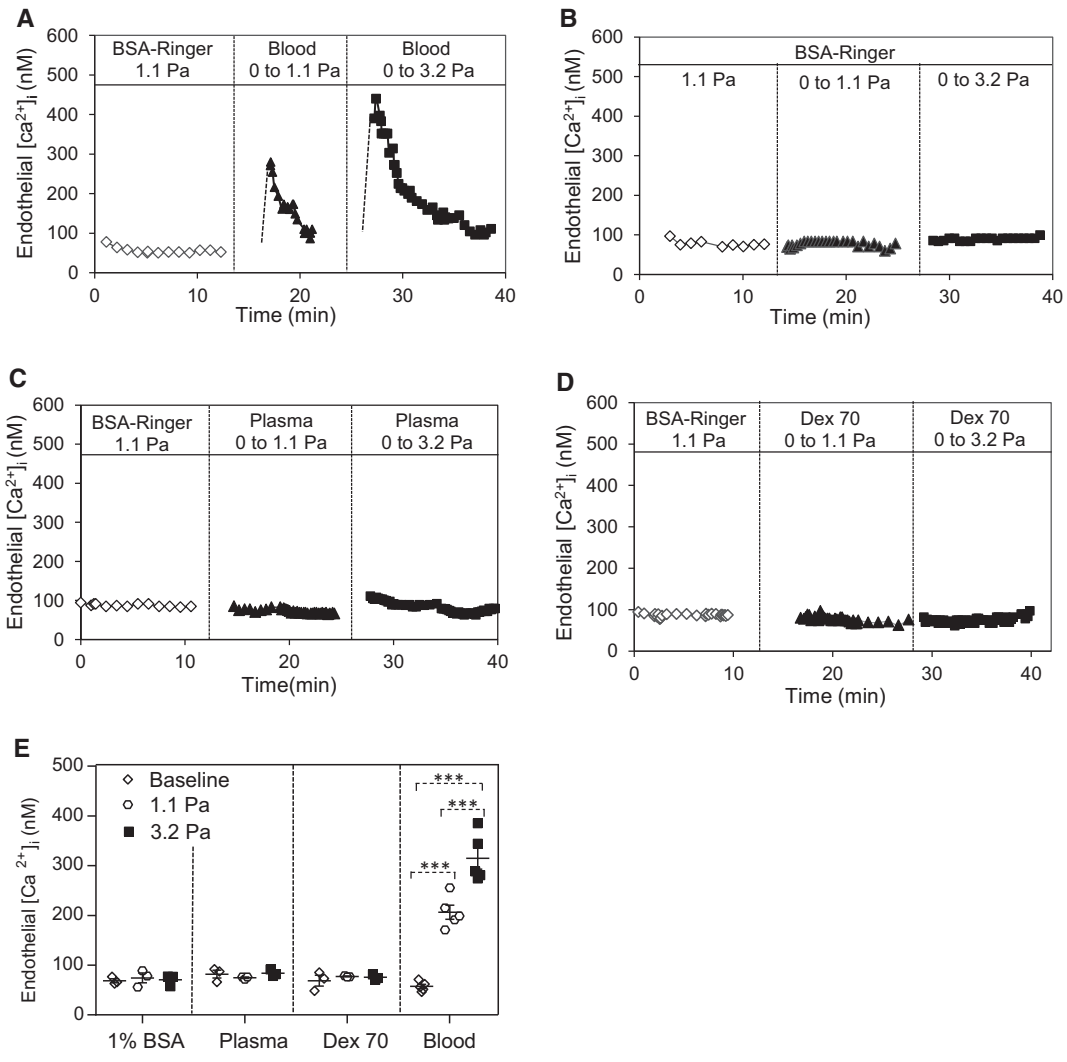

Figure 2 Blood flow generated-SS induced transient increases in EC $[Ca^{2+}]_i$ in rat venules. (*A*) SS-dependent increases in EC $[Ca^{2+}]_i$ in a blood perfused vessel. (*B–D*) The same magnitude of changes in SS did not increase EC $[Ca^{2+}]_i$ in BSA-Ringer, plasma, and 10% Dextran70 perfused vessels. (*E*) Summary results of SS-induced changes in EC $[Ca^{2+}]_i$ with different perfusate ($n = 5$ blood group, $n = 3$ other groups) ***$P < 0.0005$. Dotted line link: paired student's *t*-test for paired studies conducted in each vessel.

estimated wall SS when the RBCs passed through a perfusion pipette with a narrower tip (10 × 30 μm) than the vessel diameter, and the dynamic motions of RBCs during the flow changes may alter the applied mechanical stress,[10] which counteract the overestimation of apparent viscosity. Nevertheless, these factors only affect the precision of the estimated SS value and not the conclusions derived from the results.

3.2 Only blood flow generated SS induces transient increases in EC $[Ca^{2+}]_i$ in intact venules

The changes in EC $[Ca^{2+}]_i$ in response to changing wall SS in intact venules were measured with different perfusates. The mean EC $[Ca^{2+}]_i$ was 57 ± 4 nM when the vessel was perfused with albumin-Ringer's solution at 1.1 Pa steady SS. Then the same vessel was recannulated with a micropipette containing whole blood. When the SS was increased from 0 to 1.1 Pa or 3.2 Pa, EC $[Ca^{2+}]_i$ transiently increased to 206 ± 14 nM and 315 ± 22 nM, respectively ($n = 5$ per group). *Figure 2A* shows the changes in EC $[Ca^{2+}]_i$ from a representative experiment. However, the identical changes in SS utilizing albumin-Ringer's solution, plasma, or 10% Dextran70 perfusate did not cause increases in EC $[Ca^{2+}]_i$ (*Figure 2B–D*).

3.3 Both blood and plasma perfused venules show the shear-dependent EC NO production

SS-induced NO release from ECs is one of the important factors in the regulation of vascular function. In this study, we investigated the NO responses to the changes in SS in both blood and plasma perfused vessels. Using the NO-indicator, DAF-2, and fluorescence imaging, we found that changes of SS induced magnitude-dependent increases in NO production in both plasma and whole blood perfused vessels. When the SS increased from 0 to 1.1 and 0 to 3.2 Pa, the NO production rate was 0.36 ± 0.02 and 0.74 ± 0.10 AU/min in plasma perfused vessels, and

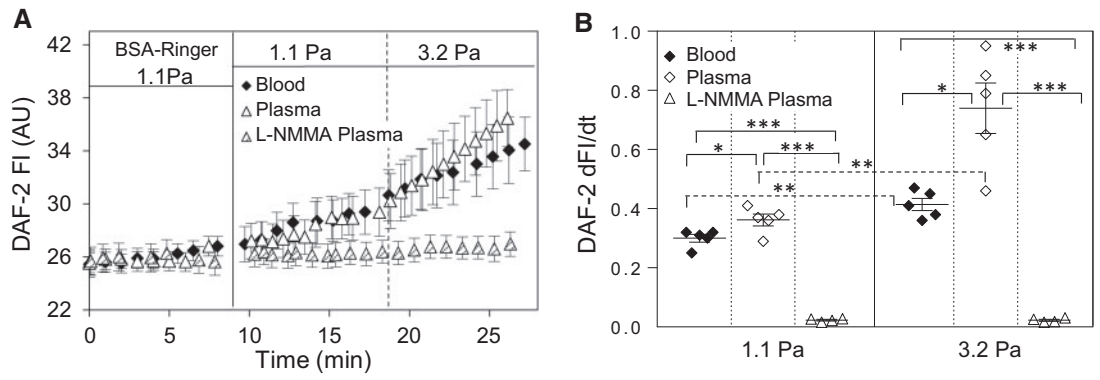

Figure 3 SS-induced EC NO production in rat venules. (*A*) Both plasma and blood perfused vessels show SS-dependent increases in EC NO production, and the application of NOS inhibitor, L-NMMA, abolished such effect. (*B*) Summary data show SS-dependent NO production rate in the absence ($n = 5$ per group) and presence of L-NMMA ($n = 4$). ***$P \leq 0.0005$, **$P < 0.005$, *$P < 0.05$. Solid line link: one-way ANOVA with post-hoc Tukey to compare perfusion groups with the same SS. Dotted line link: paired student's *t*-test for paired studies conducted in each vessel.

0.30 ± 0.01 and 0.41 ± 0.02 AU/min in blood perfused vessels ($n = 5$ per group, *Figure 3A, B*). The lower rate of the increases in NO in blood-perfused vessels as compared to plasma perfused vessels could be caused by the scavenging of NO by RBCs. To validate the increased DAF FI as an indication of NO production, a NOS inhibitor, L-NMMA, was applied to four plasma perfused vessels. The presence of L-NMMA (0.5 mM) completely abolished SS-induced NO production.

3.4 SS-induced eNOS activation

To correlate SS-induced NO production with eNOS activation status, we examined eNOS phosphorylation at Serine 1177 and Threonine 495 under the same experimental conditions as those in which NO was measured using immunofluorescence staining and confocal imaging ($n = 3$ or 4 per group). The levels of SS-induced eNOS-Ser^{1177} phosphorylation were similar in blood and plasma perfused vessels (*Figure 4A, D*). However, SS-dependent eNOS-Thr^{495} dephosphorylation only occurred in blood perfused vessels, and no significant changes were found in plasma perfused vessels (*Figure 4B, E*).

3.5 ATP released from RBCs is responsible for SS-induced transient increases in EC $[Ca^{2+}]_i$ in individually perfused venules

One of the major differences between whole blood and plasma perfused vessels is the presence of blood cells. We first examined if the presence of RBCs contributes to SS-induced changes in EC $[Ca^{2+}]_i$. Results of five experiments showed that perfusion of vessels with 40% (volume) of RBCs in albumin-Ringer perfusate resulted in similar SS-induced changes in EC $[Ca^{2+}]_i$ to those in whole blood perfused vessels. EC $[Ca^{2+}]_i$ transiently increased from a mean value of 72 ± 4 to 210 ± 8 nM and 304 ± 18 nM when wall SS increased from 0 Pa to 1.1 Pa and 3.2 Pa, respectively (*Figure 5A, E*).

We then explored the mechanisms of RBC involved SS-induced increases in EC $[Ca^{2+}]_i$. Studies have indicated that RBCs release ATP in response to shear through a pannexin 1 channel.[10,29] The SS-induced ATP release from RBCs was then measured using luciferin/luciferase assay. *Figure 5B* shows shear magnitude-dependent release of ATP from RBCs, and a pannexin 1 inhibitor, carbenoxolone (CBX, 100 μM), blocked the release of ATP ($n = 5$ per group). Most importantly, when microvessels were perfused with CBX treated RBCs, SS-induced increases in EC $[Ca^{2+}]_i$ were abolished. The mean EC $[Ca^{2+}]_i$ were 70 ± 14 and 75 ± 15 nM when SS was increased from 0 to 1.1 Pa and 3.2 Pa, respectively ($n = 5$, *Figure 5E*). In two of the five experiments, the SS-induced changes in EC $[Ca^{2+}]_i$ were measured with sequential perfusions of normal and CBX-treated RBCs in the same vessel (*Figure 5A*). The results were consistent with those conducted separately, which further support SS-induced release of ATP through pannexin 1 channel in RBCs to be responsible for SS-induced increases in EC $[Ca^{2+}]_i$. We also examined the effects of CBX and applied ATP on ECs. Results showed that directly applied ATP (10 μM) induced similar changes in EC $[Ca^{2+}]_i$ to those observed in blood or RBC perfused vessels upon changes of SS, and perfusion of vessels with CBX in the absence of RBCs affected neither baseline EC $[Ca^{2+}]_i$ nor ATP-induced increases in EC $[Ca^{2+}]_i$ (*Figure 5C, E*, $n = 4$). The possibility of platelet released ATP in response to SS was also evaluated. The ATP levels were very low (3–10 nM) in platelet rich plasma and showed no responses to applied SS ($n = 3$ per group, *Figure 5B*).

Springosine-1-phosphate (S1P) was found to be present in both plasma and solutions containing RBCs and play important roles in the regulation of microvessel permeability.[30,31] Perfusing vessels with exogenous S1P (1 μM) has been shown to increase EC $[Ca^{2+}]_i$ through S1P receptor 1 ($S1P_{R1}$) without increasing microvessel permeability.[32] To examine the potential roles of S1P in SS-induced increases in EC $[Ca^{2+}]_i$ when RBCs were present, we measured EC $[Ca^{2+}]_i$ in the presence of a $S1P_{R1}$ inhibitor, W146 (10 μM), in RBC perfused vessels. Results showed that W146 did not affect SS-induced increases in EC $[Ca^{2+}]_i$ in RBC perfused vessels. When SS increased from 0 to 1.1 and 3.2 Pa, EC $[Ca^{2+}]_i$ increased from 57 ± 4 to 222 ± 13 nM and 374 ± 50 nM, respectively, not significantly different from the responses in the absence of W146 ($n = 4$, *Figure 5E*). In contrast, W146 blocked the S1P effect on EC $[Ca^{2+}]_i$ and removal of W146 recovered the action of S1P (1 μM) with EC $[Ca^{2+}]_i$ increased from 60 ± 5 to 268 ± 52 nM ($n = 5$). The time courses of two individual experiments are superimposed in *Figure 5D*, demonstrating that the endogenous S1P in RBC perfusate does not play a role in SS-induced increases in EC $[Ca^{2+}]_i$.

The role of pannexin 1 channel in SS-induced release of ATP from RBCs was further investigated in RBCs isolated from wild type ($n = 5$) and pannexin 1 deficient mice ($n = 3$). The levels of SS-dependent release

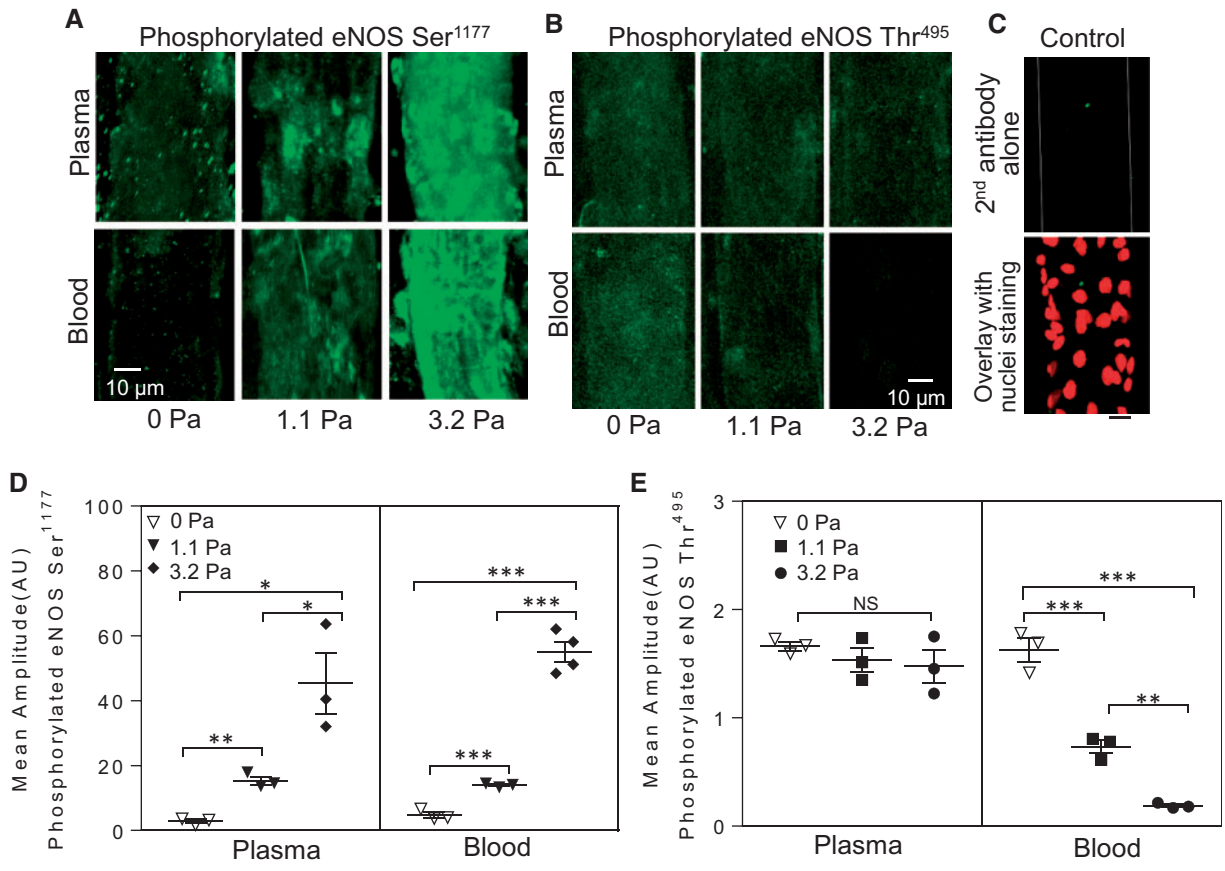

Figure 4 SS-induced eNOS activation in blood and plasma perfused vessels. (*A*) Confocal images show SS-dependent phosphorylation of eNOS-Ser^{1177} in both blood and plasma-perfused vessels. (*B*) SS-dependent dephosphorylation of eNOS-Thr^{495} occurred only in blood perfused vessels. (*C*) Negative control of second antibody alone (green, top) and overlay with labelled nuclei (DRAQ5, red, lower image). (*D* and *E*) Summary of the fluorescence quantifications ($n = 3$ or 4 per group). ***$P < 0.0005$, **$P \leq 0.005$, *$P < 0.05$, NS: $P > 0.05$ (One-way ANOVA or nested ANOVA with post-hoc Tukey).

of ATP from RBCs of wild type mice were similar to that observed in rats, but significantly diminished in RBCs of pannexin 1 deficient mice (*Figure 6A*). Meanwhile, perfusion of rat venules with albumin-Ringer perfusate containing 40% (volume) wild type mouse RBCs showed a similar pattern of shear-induced increases in EC $[Ca^{2+}]_i$ to those in rat RBC perfused vessels. EC $[Ca^{2+}]_i$ transiently increased to 231 ± 37 and 319 ± 50 nM when wall SS increased from 0 Pa to 1.1 Pa and 3.2 Pa, respectively, while the same magnitude changes in SS did not increase EC $[Ca^{2+}]_i$ in pannexin1 deficient RBC perfused vessels, and the mean EC $[Ca^{2+}]_i$ was 67 ± 6 nM and 67 ± 12 nM, respectively (*Figure 6B*).

3.6 SS-induced endothelial gap formation

Our previous study demonstrated that the magnitude of the accumulation of FMs at junctions between ECs directly correlated with the degree of endothelial gap formation and increased microvessel permeability.[25] To determine if the change of SS results in increased microvessel permeability, FMs (100 nm) were added to the blood or plasma perfusate to mark endothelial gaps upon changing SS. We found that only in blood perfused vessels, an increase of SS from 0 to 3.2 Pa induced a significant accumulation of perfused FMs at endothelial junctions and the FI of accumulated FMs was 5.1 ± 0.5 times the 0 Pa control ($n = 6$). The identical experimental procedures performed in plasma perfused vessels showed no such effect. RBC solutions (40% haematocrit) showed similar effects to blood perfused vessels, with the FI of accumulated FMs being 6.9 ± 1.1 times the 0 Pa control ($n = 5$). When the vessels were perfused with 40% CBX-treated RBCs, the FI of accumulated FMs was significantly decreased to 1.5 ± 0.1 times the 0 Pa control value ($n = 6$). *Figure 7* shows representative images and the results summary.

4. Discussion

The novel information derived from this study is that dynamic changes in blood flow alter microvascular EC function not only through wall SS, but also by shear-induced release of ATP from RBCs, and each component induces different EC signalling and affects vascular function differently. An increase in wall SS in the absence of RBCs increases EC NO production, without effect on endothelial $[Ca^{2+}]_i$. However, in blood perfused vessels, the increased SS exerted on RBCs induces shear dependent release of ATP, which increases EC $[Ca^{2+}]_i$, resulting in endothelial gap formation, an indication of increased microvessel permeability. These results provide new insights into how changes in blood flow affect microvessel function *in vivo*.

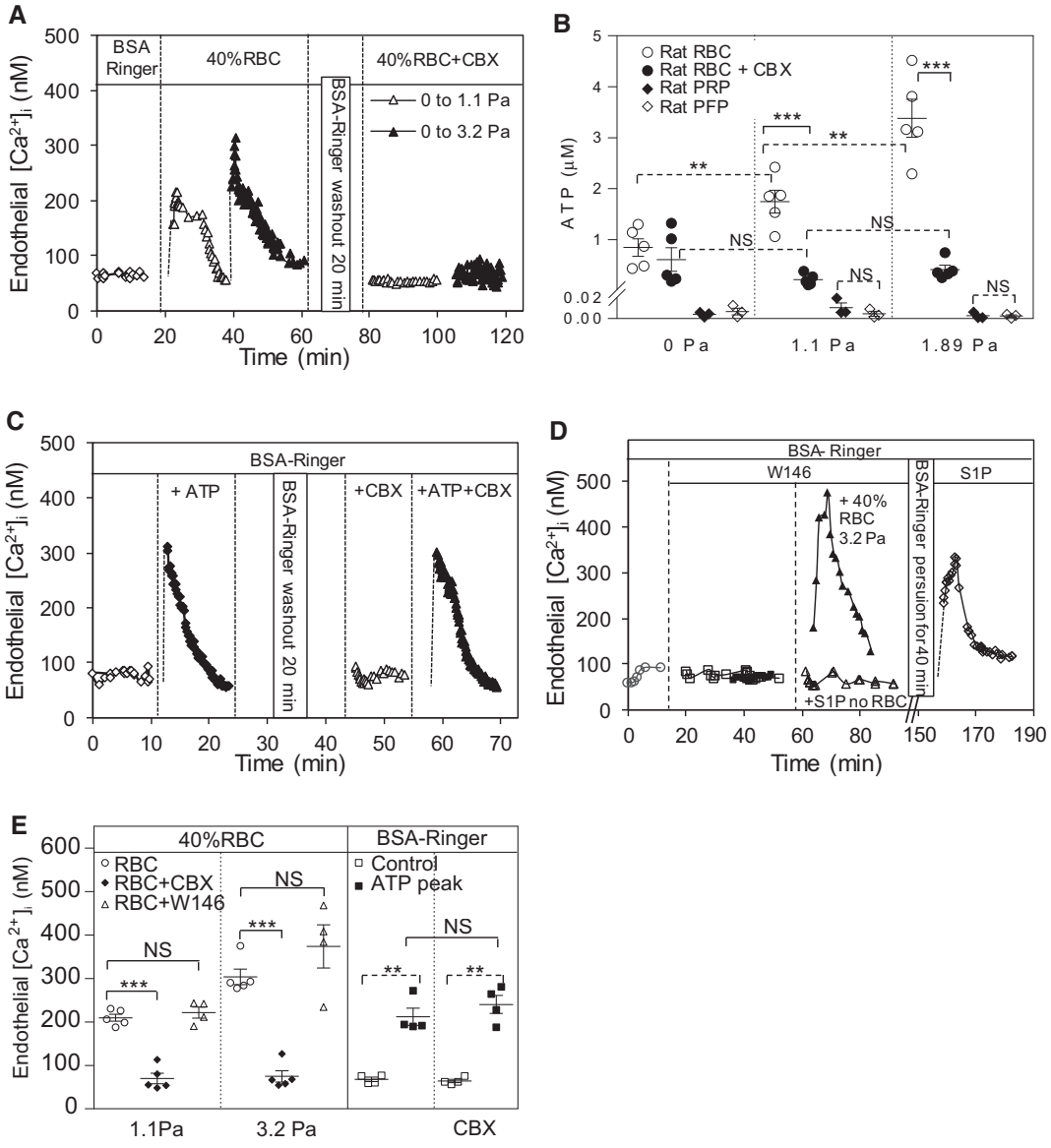

Figure 5 ATP released from RBCs contributes to SS-induced increases in EC $[Ca^{2+}]_i$ in individually perfused venules. (*A*) A representative experiment showing shear-dependent increases in EC $[Ca^{2+}]_i$ when the vessel was perfused with RBC solution (40% RBCs in albumin Ringer solution), and pre-treatment of RBCs with a pannexin 1 inhibitor, CBX (100 μM) abolished such effect. (*B*) Summary results of SS induced release of ATP from RBCs or platelets. RBCs released ATP in a shear-dependent manner, and CBX treatment abolished SS-induced ATP release from RBCs ($n = 5$ per group). ATP measured in platelet rich plasma (PRP) showed no difference from platelet free plasma (PFP) and no responses to applied SS ($n = 3$ per group). (*C*) A representative experiment showing that the applied ATP (10 μM) induced a transient increase in EC $[Ca^{2+}]_i$, and the presence of CBX (100 μM) in the perfusate did not affect baseline and ATP induced increases in EC $[Ca^{2+}]_i$. (*D*) Superimposed two individual experiments showing W146 (10 μM), a selective $S1P_{R1}$ antagonist, had no effect on baseline and SS-induced increases in EC $[Ca^{2+}]_i$ in RBC perfused vessels, but abolished S1P-induced increases in EC $[Ca^{2+}]_i$ in BSA-Ringer perfused vessels. The S1P effect was recovered after removal of W146 with 40 min perfusion of albumin-Ringer. (*E*) Summary results of EC $[Ca^{2+}]_i$ measurements ($n = 4$ or 5 per group). ***$P < 0.0005$, **$P < 0.005$, NS: $P > 0.05$. Solid line link: one-way ANOVA with post-hoc Tukey for perfusion groups with the same SS, and unpaired student's *t*-test for two group comparison. Dotted line link: paired student's *t*-test for paired studies conducted in each vessel or animal.

4.1 Mechanisms of SS-induced increases in EC $[Ca^{2+}]_i$: the role of shear-induced release of ATP from RBCs

It has been controversial for decades whether the changes of vascular flow are accompanied by elevated EC cytoplasmic $[Ca^{2+}]_i$.[7,8,18,19] Studies that report flow-induced increases in EC $[Ca^{2+}]_i$ were mainly conducted in cultured ECs in the absence of blood components, and ATP release from ECs has been a focus.[2–5] However, the reported flow-induced ATP release from cultured ECs were all in nanomolar concentration ranges.[2–5] Based on EC $[Ca^{2+}]_i$ measurements with directly applied ATP in intact microvessels, or in cultured ECs,[5] micromolar

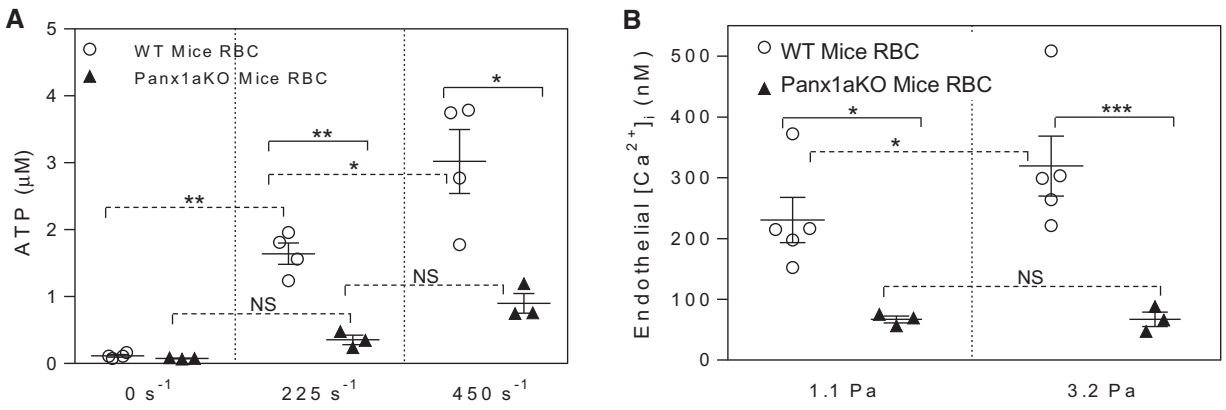

Figure 6 Role of RBC pannexin 1 (Panx1) channel in SS-induced release of ATP. (*A*) Summary of SS-induced release of ATP from RBCs from wild type and Panx1 deficient mice. (*B*) Summary data show that genetic removal of Panx1 channels that abolished SS-induced ATP release also prevented SS-induced increases in EC $[Ca^{2+}]_i$ ($n = 5$ for wild type group, $n = 3$ for Panx1 knockdown group). ***$P < 0.0005$, **$P < 0.005$, *$P < 0.05$, NS: $P > 0.05$. Solid line link: unpaired student's *t*-test between two groups. Dotted line link: paired student's *t*-test for paired studies in each vessel or animal.

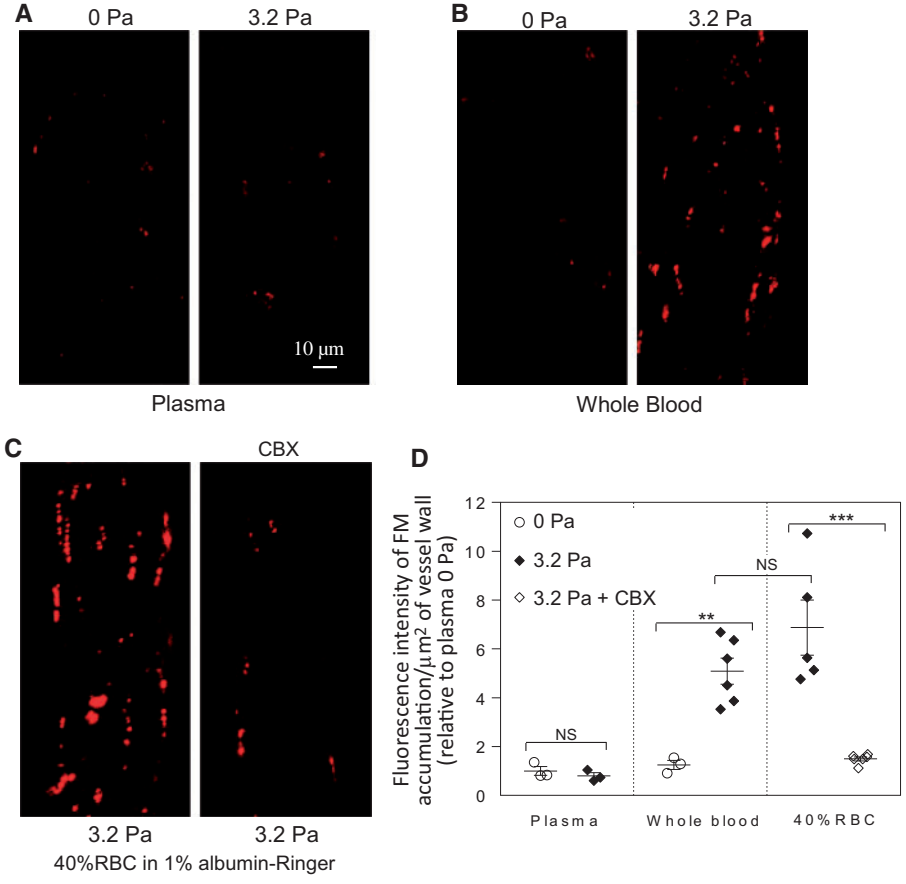

Figure 7 SS-induced release of ATP from RBCs causes EC gap formation in intact venules. (*A* and *B*) Confocal images show the differences of fluorescence microsphere (FM) accumulation at junctions between ECs in response to the same magnitude changes in SS between plasma and blood perfused vessels. (*C*) The changes of SS-induced accumulation of FMs were significantly attenuated when the vessel was perfused with CBX pre-treated RBCs (40% haematocrit). (*D*) Quantification of the FI of accumulated FMs at endothelial junctions. ($n = 3$ for plasma and blood 0 Pa; $n = 6$ for blood 3.2 Pa and 40% RBC + CBX; $n = 5$ for 40% RBC 3.2 Pa). ***$P < 0.0005$, **$P < 0.005$, NS: $P > 0.05$ (One-way ANOVA with post-hoc Tukey for different perfusion groups under the same SS, and unpaired student's *t*-test for two group comparisons).

concentrations of ATP are required to sufficiently increase EC $[Ca^{2+}]_i$ and affect EC function. The flow-induced Ca^{2+} changes observed in cultured ECs could be the result of exposing a well-adapted static culture conditions to a flow, or differences in phenotype and sensitivity to stimuli between ECs in culture and in intact vessels.[9]

RBCs, the major cellular components in the blood, have been reported to release ATP in response to reduced oxygen tension.[33] *In vitro* studies using microfluidic approaches or microbore tubing have reported that increased SS or cell deformation also induces the release of ATP from RBCs.[11,12] But SS-induced release of ATP from RBCs has not previously been incorporated into studies of SS-induced changes in EC functions. Recently pannexin 1, a gap junction protein, has been proposed to form a mechanosensitive and ATP-permeable channel in the non-junctional plasma membrane.[29,34] Consistent with a role of pannexin 1 as a mechanosensitive ATP release channel, we and others[10,29] showed that a gap junction blocker, CBX, or genetic removal of pannexin 1 channel significantly attenuated the SS-induced ATP release from RBCs. Our study demonstrates that the levels of SS-induced release of ATP from RBCs at physiological haematocrits are in the micromolar concentration range, about 3 orders of magnitude higher than those from ECs in culture.[2–5] However, the impact of this important source of ATP from RBCs on ECs during changes in SS has been overlooked for decades. Our study provides the first evidence that RBCs contribute a significant source of ATP when blood flow changes and play an essential role in EC signalling and the regulation of vascular function. Importantly, our experimental approach enables us to differentiate the contributions of different sources of ATP to EC signalling and the regulation of barrier function in intact microvessels. The results demonstrate that the micromolar concentrations of released ATP by RBCs in response to changes of SS increase EC $[Ca^{2+}]_i$ and result in EC gap formation in intact microvessels. In contrast, in the absence of RBCs, i.e. in plasma or dextran 70 perfused vessels, or when RBC released ATP was blocked, the same magnitude of changes in SS did not initiate EC Ca signalling or affect EC barrier function. This indicates that EC released ATP alone is insufficient to increase EC $[Ca^{2+}]_i$ in intact microvessels. We also only detected nanomolar concentrations of ATP in sheared platelet rich plasma, indicating that platelets are not a significant source of ATP when blood flow changes.

4.2 SS-induced EC NO production and eNOS activation

Although it has been well-recognized that the changes of SS induce NO production from ECs, the signalling mechanisms remain contradictory. Some *in vitro* studies reported that SS-induced NO was independent of external Ca^{2+}, but mediated by Ca^{2+} release from intracellular stores.[35] Others reported that extracellular Ca^{2+} is required for flow-induced NO.[36,37] There are also studies reporting that flow-induced NO or vasodilation of coronary arterioles occurs through a Ca^{2+}-insensitive pathway.[18] Our results indicated that SS-induced NO synthesis can be independent of increases in EC $[Ca^{2+}]_i$, since the increased NO production in response to SS occurred not only in blood perfused vessels, but also in plasma-perfused vessels, and the latter do not involve in the increases in EC $[Ca^{2+}]_i$. The SS-induced NO was assessed by DAF-2 fluorescence in preloaded microvessels. Although some specificity issues of DAF-2 have been raised,[38] based on our experience and experimental results, DAF-2 is still a better tool than other available approaches for assessment of intracellular NO, if the probe concentration, experimental procedure, and data analysis are handled properly.[23] Our previous studies have been able to detect a large range of NO production rates from basal to different stimulated levels in ECs of intact microvessels.[23,24,39] In this study, the result that the application of LNMMA in a plasma perfused vessel completely abolished SS-induced increases in DAF-2 FI (*Figure 3A*) supports the interpretation that the slope changes in DAF-2 FI reflect the rate of NO synthesis.

Our study also showed a close correlation between SS-induced NO production measured with NO indicator DAF-2 with eNOS phosphorylation status using immunofluorescence staining and confocal imaging in individual vessels. While western blot is the conventional approach to evaluate protein activation status in cultured cells with one cell type, it is not suited for individually perfused microvessels. The dissected tissue, regardless of dissection technique, will have mixed cell types, and only a very small portion will be ECs exposed to the defined changes of SS. Therefore, the results derived from homogenized tissue with western blot will not be specific for eNOS status of ECs in the perfused microvessels. The immunostaining in individually perfused microvessels offers unique advantages over western blot for individual vessel studies. It allowed us to assess the activation status of a specific protein with temporal and spatial resolution in ECs of the vessel walls. Our current and previous studies using the immunostaining approach have demonstrated a well-correlated relationship between EC eNOS phosphorylation status and NO production rate in response to different stimuli.[24] Cultured EC and isolated protein studies indicated that eNOS phosphorylation at Ser^{1177} represents a Ca^{2+}-independent regulatory mechanism for NO production,[40] while the dephosphorylation of Thr^{495}-associated eNOS activation depends on increased EC $[Ca^{2+}]_i$.[41] Our results that SS-induced eNOS-Ser^{1177} phosphorylation occurred in both plasma and whole blood perfused vessels, and SS-induced eNOS-Thr^{495} dephosphorylation only occurred in blood perfused microvessels, are consistent with the molecular regulatory characterization of eNOS activation sites. These results further support our hypothesis that the changes in wall SS in the absence of RBCs activate eNOS via a Ca^{2+}-independent mechanism; while in the presence of RBCs, the SS-induced activation of eNOS involves both Ca^{2+} dependent and independent mechanisms, and Ca^{2+} dependent eNOS activation is the result of ATP-mediated increases in EC $[Ca^{2+}]_i$ and dominated by RBC released ATP. Although some studies indicate that eNOS exists in RBCs and produce NO, their functional significance appears limited, because oxygenated haemoglobin is a highly efficient NO scavenger.[42] Our NO measurements in blood perfused vessels is consistent with this notion.

4.3 SS and microvessel permeability

Although studies in individually perfused microvessels in both frog and rat mesenteries have demonstrated flow-dependent increases in permeability to small solutes, such as K^+ and sodium fluorescein,[20,43] the results of flow-induced changes in permeability to macromolecules and fluid (Lp) remain contradictory.[15–17,44] It is a technical challenge to quantitatively measure SS-induced hydraulic permeability following the traditional single vessel perfusion and occlusion technique.[22] To date, studies using single vessel perfusion techniques were all conducted in the absence of a significant number of RBCs (about 1% RBCs were commonly used as velocity markers), and therefore assess relatively cell-free fluid generated wall SS. To overcome the technical difficulties of assessing SS-induced permeability to fluid and macromolecules in the presence of RBCs, we directly evaluated EC junctional changes in response to changed SS using FMs as markers.[25] We have demonstrated that when FMs (100 nm diameter) were perfused into platelet activating factor (PAF) stimulated rat venules, the number of FMs accumulated at EC

junctions represented the extent of gap formation between ECs (validated by electron microscopy), and were temporally correlated with the time course of PAF-induced Lp changes.[25] Using this method, we have now discovered that changes of SS in cell-free fluid perfused vessels had no effect on EC junctions, and only in the presence of significant quantities of RBCs did the changes of SS induce EC gap formation and an increase in microvessel permeability. Significantly, the EC junctional accumulation of FMs was abolished when RBC released ATP was inhibited by a pannexin 1 inhibitor, supporting that endothelial gap formation is directly linked to RBC released ATP and ATP-induced increases in EC $[Ca^{2+}]_i$. SS-induced NO production alone (in the absence of RBC released ATP) showed no effect on EC $[Ca^{2+}]_i$ or EC gap formation. These results further support the mechanism of Ca^{2+}-dependent regulation of microvessel permeability.[9,22] The endothelial glycocalyx has been suggested to play important roles in mechanosensing and vascular permeability control.[6] We do not anticipate a significant modification of glycocalyx to be associated with EC gap formation as the results of changing SS under our experimental conditions. If changes in glycocalyx occurred, it must be attributed to its quick reaction to RBC released ATP, and not the applied SS, since the same magnitude changes in SS did not induce increases in EC $[Ca^{2+}]_i$ and gap formation in plasma perfused vessels. Endogenous springosine-1-phosphate (S1P) that presents in both blood and plasma may also affect EC function.[30,31] However, the main actions of S1P on ECs are to strengthen junctions between ECs and prevent stimuli-induced EC gap formation,[30–32] which are opposite from SS induced EC gap formation in the presence of RBCs. In addition, our results that inhibition of $S1P_{R1}$ with W146 blocked S1P effects on EC $[Ca^{2+}]_i$ without affecting SS-induced increases in EC $[Ca^{2+}]_i$ do not support a role of S1P in SS-induced responses. The SS-induced release of ATP from RBCs may contribute to vasodilation in arterioles under certain conditions, but may also play a role in sensitizing ECs to inflammatory stimuli and accelerating pathological processes under disease conditions.

5. Conclusions

Our study demonstrates that changes in blood flow can alter microvascular EC function through both wall SS and shear-induced release of ATP from RBCs, and that the released ATP from RBCs plays an important role in altering EC barrier integrity and vascular permeability. Our findings that derived from intact venules could also apply to different vasculatures and explain why certain vascular regions exposed to altered mechanical forces are prone to inflammation, manifesting higher sensitivity for leucocyte adhesion in venules and atherosclerotic plaque formation in large arteries under pathological conditions. Consistent with this hypothesis, experiments with pannexin $1^{-/-}$ and pannexin $2^{-/-}$ mice reported a better functional outcome and smaller infarcts than wild-type mice when subjected to ischemic stroke[45] and to ischemia-induced retinal ganglion cell death.[46] The new mechanistic insight provided by this study may benefit targeted therapeutic development for mechanical force-involved vascular dysfunction under pathological conditions.

Supplementary material

Supplementary material is available at *Cardiovascular Research* online.

Acknowledgements

The authors thank Dr Howard A. Stone (Princeton University) for his valuable input about shear stress on red blood cells and results interpretations, and Dr Herbert Lipowsky (Pennsylvania State University) for his comments about apparent viscosity.

Conflict of interest: none declared.

Funding

This work was supported by National Heart, Lung, and Blood Institute HL56237, HL084338, HL130363 and National Institute of Diabetes and Digestive and Kidney Diseases DK097391 (to H.P.); and American Heart Association Great Rivers Affiliate pre-doctoral fellowship [12PRE11470010 to X.S.]. NIH HL128563 to S.H.

References

1. Stone PH, Coskun AU, Kinlay S, Clark ME, Sonka M, Wahle A, Ilegbusi OJ, Yeghiazarians Y, Popma JJ, Orav J, Kuntz RE, Feldman CL. Effect of endothelial shear stress on the progression of coronary artery disease, vascular remodeling, and in-stent restenosis in humans: in vivo 6-month follow-up study. *Circulation* 2003;**108**:438–444.
2. Bodin P, Bailey D, Burnstock G. Increased flow-induced ATP release from isolated vascular endothelial cells but not smooth muscle cells. *Br J Pharmacol* 1991;**103**:1203–1205.
3. Bodin P, Burnstock G. Purinergic signalling: ATP release. *Neurochem Res* 2001;**26**:959–969.
4. Wang S, Chennupati R, Kaur H, Iring A, Wettschureck N, Offermanns S. Endothelial cation channel PIEZO1 controls blood pressure by mediating flow-induced ATP release. *J Clin Invest* 2016;**126**:4527–4536.
5. Wang S, Iring A, Strilic B, Albarran Juarez J, Kaur H, Troidl K, Tonack S, Burbiel JC, Muller CE, Fleming I, Lundberg JO, Wettschureck N, Offermanns S. P2Y(2) and Gq/G(1)(1) control blood pressure by mediating endothelial mechanotransduction. *J Clin Invest* 2015;**125**:3077–3086.
6. Tarbell JM, Simon SI, Curry FR. Mechanosensing at the vascular interface. *Annu Rev Biomed Eng* 2014;**16**:505–532.
7. Mendoza SA, Fang J, Gutterman DD, Wilcox DA, Bubolz AH, Li R, Suzuki M, Zhang DX. TRPV4-mediated endothelial Ca2+ influx and vasodilation in response to shear stress. *Am J Physiol Heart Circ Physiol* 2010;**298**:H466–H476.
8. Geiger RV, Berk BC, Alexander RW, Nerem RM. Flow-induced calcium transients in single endothelial cells: spatial and temporal analysis. *Am J Physiol* 1992;**262**:C1411–C1417.
9. Curry FR, Adamson RH. Vascular permeability modulation at the cell, microvessel, or whole organ level: towards closing gaps in our knowledge. *Cardiovasc Res* 2010;**87**:218–229.
10. Forsyth AM, Wan J, Owrutsky PD, Abkarian M, Stone HA. Multiscale approach to link red blood cell dynamics, shear viscosity, and ATP release. *Proc Natl Acad Sci USA* 2011;**108**:10986–10991.
11. Wan J, Ristenpart WD, Stone HA. Dynamics of shear-induced ATP release from red blood cells. *Proc Natl Acad Sci USA* 2008;**105**:16432–16437.
12. Edwards J, Sprung R, Sprague R, Spence D. Chemiluminescence detection of ATP release from red blood cells upon passage through microbore tubing. *Analyst* 2001;**126**:1257–1260.
13. Sprague RS, Ellsworth ML, Stephenson AH, Lonigro AJ. ATP: the red blood cell link to NO and local control of the pulmonary circulation. *Am J Physiol* 1996;**271**:H2717–H2722.
14. Price AK, Martin RS, Spence DM. Monitoring erythrocytes in a microchip channel that narrows uniformly: towards an improved microfluidic-based mimic of the microcirculation. *J Chromatogr A* 2006;**1111**:220–227.
15. Neal CR, Bates DO. Measurement of hydraulic conductivity of single perfused Rana mesenteric microvessels between periods of controlled shear stress. *J Physiol* 2002;**543**:947–957.
16. Williams DA. A shear stress component to the modulation of capillary hydraulic conductivity (Lp). *Microcirculation* 1996;**3**:229–232.
17. Adamson RH, Sarai RK, Altangerel A, Clark JF, Weinbaum S, Curry FE. Microvascular permeability to water is independent of shear stress, but dependent on flow direction. *Am J Physiol Heart Circ Physiol* 2013;**304**:H1077–H1084.
18. Muller JM, Davis MJ, Kuo L, Chilian WM. Changes in coronary endothelial cell Ca2+ concentration during shear stress- and agonist-induced vasodilation. *Am J Physiol* 1999;**276**:H1706–H1714.
19. Ungvari Z, Sun D, Huang A, Kaley G, Koller A. Role of endothelial [Ca2+]i in activation of eNOS in pressurized arterioles by agonists and wall shear stress. *Am J Physiol Heart Circ Physiol* 2001;**281**:H606–H612.
20. Kajimura M, Head SD, Michel CC. The effects of flow on the transport of potassium ions through the walls of single perfused frog mesenteric capillaries. *J Physiol* 1998;**511** (pt. 3):707–718.

21. Zweifach BW, Lipowsky HH. Quantitative studies of microcirculatory structure and function. III. Microvascular hemodynamics of cat mesentery and rabbit omentum. *Circ Res* 1977;**41**:380–390.
22. He P, Zhang X, Curry FE. Ca2+ entry through conductive pathway modulates receptor-mediated increase in microvessel permeability. *Am J Physiol* 1996;**271**:H2377–H2387.
23. Zhou X, He P. Improved measurements of intracellular nitric oxide in intact microvessels using 4,5-diaminofluorescein diacetate. *Am J Physiol Heart Circ Physiol* 2011;**301**:H108–H114.
24. Zhou X, Yuan D, Wang M, He P. H2O2-induced endothelial NO production contributes to vascular cell apoptosis and increased permeability in rat venules. *Am J Physiol Heart Circ Physiol* 2013;**304**:H82–H93.
25. Jiang Y, Wen K, Zhou X, Schwegler-Berry D, Castranova V, He P. Three-dimensional localization and quantification of PAF-induced gap formation in intact venular microvessels. *Am J Physiol Heart Circ Physiol* 2008;**295**:H898–H906.
26. Lipowsky HH, Kovalcheck S, Zweifach BW. The distribution of blood rheological parameters in the microvasculature of cat mesentery. *Circ Res* 1978;**43**:738–749.
27. Pries AR, Neuhaus D, Gaehtgens P. Blood viscosity in tube flow: dependence on diameter and hematocrit. *Am J Physiol* 1992;**263**:H1770–H1778.
28. Secomb TW. Flow-dependent rheological properties of blood in capillaries. *Microvasc Res* 1987;**34**:46–58.
29. Locovei S, Bao L, Dahl G. Pannexin 1 in erythrocytes: function without a gap. *Proc Natl Acad Sci USA* 2006;**103**:7655–7659.
30. Adamson RH, Clark JF, Radeva M, Kheirolomoom A, Ferrara KW, Curry FE. Albumin modulates S1P delivery from red blood cells in perfused microvessels: mechanism of the protein effect. *Am J Physiol Heart Circ Physiol* 2014;**306**:H1011–H1017.
31. Curry FE, Clark JF, Adamson RH. Erythrocyte-derived sphingosine-1-phosphate stabilizes basal hydraulic conductivity and solute permeability in rat microvessels. *Am J Physiol Heart Circ Physiol* 2012;**303**:H825–H834.
32. Zhang G, Xu S, Qian Y, He P. Sphingosine-1-phosphate prevents permeability increases via activation of endothelial sphingosine-1-phosphate receptor 1 in rat venules. *Am J Physiol Heart Circ Physiol* 2010;**299**:H1494–H1504.
33. Ellsworth ML, Ellis CG, Sprague RS. Role of erythrocyte-released ATP in the regulation of microvascular oxygen supply in skeletal muscle. *Acta Physiol (Oxf)* 2016;**216**:265–276.
34. Lohman AW, Billaud M, Isakson BE. Mechanisms of ATP release and signalling in the blood vessel wall. *Cardiovasc Res* 2012;**95**:269–280.
35. Shen J, Luscinskas FW, Connolly A, Dewey CF Jr, Gimbrone MA Jr. Fluid shear stress modulates cytosolic free calcium in vascular endothelial cells. *Am J Physiol* 1992;**262**:C384–C390.
36. Buga GM, Gold ME, Fukuto JM, Ignarro LJ. Shear stress-induced release of nitric oxide from endothelial cells grown on beads. *Hypertension* 1991;**17**:187–193.
37. Kuchan MJ, Frangos JA. Role of calcium and calmodulin in flow-induced nitric oxide production in endothelial cells. *Am J Physiol* 1994;**266**:C628–C636.
38. Jourd'heuil D. Increased nitric oxide-dependent nitrosylation of 4,5-diaminofluorescein by oxidants: implications for the measurement of intracellular nitric oxide. *Free Radic Biol Med* 2002;**33**:676–684.
39. Xu S, Zhou X, Yuan D, Xu Y, He P. Caveolin-1 scaffolding domain promotes leukocyte adhesion by reduced basal endothelial nitric oxide-mediated ICAM-1 phosphorylation in rat mesenteric venules. *Am J Physiol Heart Circ Physiol* 2013;**305**:H1484–H1493.
40. Fleming I, Busse R. Molecular mechanisms involved in the regulation of the endothelial nitric oxide synthase. *Am J Physiol Regul Integr Comp Physiol* 2003;**284**:R1–R12.
41. Fleming I, Fisslthaler B, Dimmeler S, Kemp BE, Busse R. Phosphorylation of Thr(495) regulates Ca(2+)/calmodulin-dependent endothelial nitric oxide synthase activity. *Circ Res* 2001;**88**:E68–E75.
42. Cortese-Krott MM, Kelm M. Endothelial nitric oxide synthase in red blood cells: key to a new erythrocrine function? *Redox Biol* 2014;**2**:251–258.
43. Montermini D, Winlove CP, Michel C. Effects of perfusion rate on permeability of frog and rat mesenteric microvessels to sodium fluorescein. *J Physiol* 2002;**543**:959–975.
44. Yuan Y, Granger HJ, Zawieja DC, Chilian WM. Flow modulates coronary venular permeability by a nitric oxide-related mechanism. *Am J Physiol* 1992;**263**:H641–H646.
45. Bargiotas P, Krenz A, Monyer H, Schwaninger M. Functional outcome of pannexin-deficient mice after cerebral ischemia. *Channels (Austin)* 2012;**6**:453–456.
46. Dvoriantchikova G, Ivanov D, Barakat D, Grinberg A, Wen R, Slepak VZ, Shestopalov VI. Genetic ablation of Pannexin1 protects retinal neurons from ischemic injury. *PLoS One* 2012;**7**:e31991.